Flash and Storm: Fast and Highly Practical Tone Mapping based on Naka-Rushton Equation

Nikola Banić and Sven Lončarić
Image Processing Group, Department of Electronic Systems and Information Processing,
Faculty of Electrical Engineering and Computing, University of Zagreb, 10000 Zagreb, Croatia

Keywords: HDR, Image Compression, Image Enhancement, LDR, Naka-Rushton Equation, Retinex, Tone Mapping Operator.

Abstract: Tone mapping operators (TMOs) are used to convert high dynamic range (HDR) images to their low dynamic range (LDR) versions mostly to display them on standard display devices. The problem with many TMOs that produce high-quality results is that they are too slow to be used in real-time applications. In this paper, a new TMO is proposed whose steps are primarily designed to achieve high speed and to be practically implementable. Under this constraint the secondary goal is to produce low dynamic range images of high quality. The proposed TMO is based on Naka-Rushton equation used in combination with additional improvements and it has $O(1)$ per-pixel complexity. The presented and discussed results show that, beside being faster and more practical, the proposed TMO outperforms many state-of-the-art TMOs in terms of resulting LDR image quality. To further demonstrate its practicality, the source code written in C++, Matlab, Python, Java, and HTML+JavaScript is available at http://www.fer.unizg.hr/ipg/resources/color_constancy/.

1 INTRODUCTION

The dynamic range of an image is the ratio between its largest and smallest non-zero intensity. Even though high dynamic range (HDR) images are used ever more frequently (Reinhard et al., 2010), most display devices are currently limited to show only low dynamic range (LDR) images. To display an HDR image on such devices, its dynamic range has to be compressed in the process called tone mapping by means of methods called tone mapping operators (TMOs). Tone mapping usually processes the image luminance channel, often calculated as the Y channel of the YUV colorspace. For a pixel with a given RGB representation $\mathbf{p} = (R,G,B)^T$ the value of Y is (Koschan and Abidi, 2008):

$$Y = 0.299R + 0.587G + 0.114B. \quad (1)$$

Alternative luminance channels are found in HSV, HSL, and Lab colorspaces or custom definitions (Banić and Lončarić, 2014b; Nguyen and Brown, 2017). If the luminance value L of $\mathbf{p}$ is tone mapped to L', then $\mathbf{p}$ is changed to

$$\mathbf{p}' = \frac{L'}{L}\mathbf{p} = \left(\frac{L'}{L}R, \frac{L'}{L}G, \frac{L'}{L}B\right)^T. \quad (2)$$

If a TMO processes intensities based only on their value and regardless of their location, then it is a global TMO, otherwise it is a local one. Examples of global TMOs include application of Steven's law (Tumblin and Rushmeier, 1993; Chiu et al., 1993; Ward, 1994), imitation of human response to light (Schlick, 1995; Pattanaik et al., 2000; Drago et al., 2003; Reinhard and Devlin, 2005), histogram adjustment (Larson et al., 1997), and sigmoidal contrast enhancement (Braun and Fairchild, 1999). For local TMOs examples include application of anisotropic diffusion (Tumblin and Turk, 1999), bilateral filtering of the image base layer (Durand and Dorsey, 2002), photographic practice (Reinhard et al., 2002), luminance gradient field manipulation (Fattal et al., 2002; Mantiuk et al., 2006), Retinex theory (Meylan and Susstrunk, 2006; Banić and Lončarić, 2014a; Banić and Lončarić, 2016). Global TMOs are faster and usually simpler, but local TMOs tend to give results of higher quality (Kuang et al., 2004; Kuang et al., 2007; Urbano et al., 2010). The problem with many TMOs that produce high-quality results is that they are too slow to be used in real-time applications. In this paper a new TMO is proposed whose steps are primarily designed to achieve high speed and to be practically implementable. Under this constraint

Banić, N. and Lončarić, S.
Flash and Storm: Fast and Highly Practical Tone Mapping based on Naka-Rushton Equation.
DOI: 10.5220/0006621600470053
In *Proceedings of the 13th International Joint Conference on Computer Vision, Imaging and Computer Graphics Theory and Applications (VISIGRAPP 2018) - Volume 4: VISAPP*, pages 47-53
ISBN: 978-989-758-290-5

the secondary goal is to produce low dynamic range (LDR) images of high quality. The proposed TMO is based on Naka-Rushton equation used in combination with additional improvements and it has $O(1)$ per-pixel complexity. The presented and discussed results show that, beside being faster and more practical, the proposed TMO outperforms many state-of-the-art TMOs in terms of resulting LDR image quality. To further demonstrate its practicality and simplify its usage by interested parties, the publicly available source code of the proposed TMO is written in several programming languages including JavaScript with an HTML interface so that it can be used even with only a browser.

The paper is structured as follows: in Section 2 the foundations for the new TMO are laid, in Sections 3 the TMO is extended to a local one, in Section 4 experimental results are presented and discussed, and Section 5 concludes the paper.

2 FLASH - STARTING GLOBALLY

2.1 Initial Tone Compression

Recently a high quality two-phase TMO called Puma with $O(1)$ per-pixel complexity has been proposed (Banić and Lončarić, 2016). During its first phase the actual tone compression is performed globally by means of a method called Flash. It is fast and efficient since it uses a simple to calculate curve, but the resulting LDR image is crude and of low quality. The second phase consists of enhancing this image by applying Smart Light Random Memory Sprays Retinex (SLRMSR) (Banić and Lončarić, 2015; Banić and Lončarić, 2017), a brightness adjustment method, whose parameters are set to specifically chosen values for this purpose. SLRMSR produces the final high quality LDR image and it has $O(1)$ per-pixel complexity. Despite good overall theoretical complexity, Puma is not especially fast due to a large constant number of steps per pixel used in SLRMSR. Additionally, SLRMSR has several parameters that need to be tuned for various tone mapping effects. Hence, Puma does not fully abide by the constraints laid out in the introduction. Nevertheless, if SLRMSR is left out, Flash can still be used as a good foundation for a desired new TMO because of its effectiveness, while for the enhancement of its results a more efficient method has to be found. The core of Flash is the Naka-Rushton equation (Shapley and Enroth-Cugell, 1984) given in the form

$$L' = \frac{\frac{L}{L_w}}{\frac{L}{L_w} + a} = \frac{L}{L + aL_w} \tag{3}$$

where L is the initial luminance, a is a scaling parameter, and L_w is the image key, which is usually approximated by calculating the geometric luminance mean (Ward, 1994; Reinhard et al., 2002)

$$L_w = \exp\left(\frac{1}{N}\sum_i \ln\left(L(i) + \varepsilon\right)\right) \tag{4}$$

where N is the number of pixels, $L(i)$ is the i-th pixel luminance, and ε is a small value to avoid logarithm of zero. By being a special case of the perceptually based Michaelis-Menten equation (Dowling, 1987), the Naka-Rushton equation is to some degree inherently also perceptually based, which makes Flash theoretically sound and even more attractive. To obtain high quality results, Flash uses the V channel of the HSV colorspace as the luminance channel where V is calculated as $V = \max\{R, G, B\}$. Flash$_a$ denotes the application of Flash for a given value of a.

2.2 Leap - Simple Image Enhancement

The next step is to enhance the crude results of Flash in a way that abides by the constraints laid out in the introduction. A good starting point in designing such an enhancement procedure partially motivated by (Huang and Mumford, 1999) is to look for simple properties common to many tone mapped LDR images of high quality. Once some of these properties are found, their incorporation into the results of Flash should hopefully increase their quality.

The set of high quality tone mapped LDR images needed to look for such properties was created by turning the HDR images available at (NTUST, 2015) and (Fairchild, 2015) into LDR images by using the procedure described in (Ma et al., 2015). This procedure takes an initial LDR version of a given HDR image and changes it iteratively in order to increase the value of TMQI-II (Ma et al., 2015), an adapted version of Tone Mapped image Quality Index (TMQI) (Yeganeh and Zhou, 2013) that evaluates structural fidelity and statistical naturalness of a tone mapped image by using the initial HDR image as a reference. Although the procedure is far too slow to be used in practical real-time systems, its final results are by definition of high quality. The procedure was iteratively applied to HDR images until the TMQI-II value of an image was very close to the maximum of 1 or the number of iterations reached 500.

The analysis of different properties across all of the obtained high quality LDR images has shown that the arithmetic mean of the grayscale image values is

a stable property with a low standard deviation over the images. For the first dataset (NTUST, 2015) the mean of the images' grayscale means was 100.57 with a standard deviation 3.85 and for the second dataset (Fairchild, 2015) these values were 100.04 and 5.12, respectively. This suggests that an appropriate mean grayscale value could also assure a higher quality. One of the simplest ways to achieve this is to multiply a given image by a scalar in order to obtain a desired mean grayscale value i.e. to jump from the initial mean grayscale to a given one. In Section 4.2 it is shown that such a procedure may indeed significantly increase the image quality of a given LDR image. For easier notation this procedure is named Leap$_g$ with g being the target mean grayscale. For some low key images their high intensity pixels may appear "burned" after increasing their brightness even further by applying Leap, but as explained in (Reinhard et al., 2002), this can actually be desirable. As a matter of fact, in (Reinhard et al., 2002) an extension of Eq. (3) has been proposed for exactly that purpose. The pseudocode for Leap is given in Algorithm 1. In the Section 4.2 it is shown that Flash combined with Leap is a fast and high quality global TMO.

After carrying out subjective assessment of a large number of LDR images obtained by applying Flash and Leap, it was concluded that round default values for a and g that already produce visually appealing results are 10 and 110, respectively.

Algorithm 1: Leap.

Input: image **I**, target mean grayscale g, upper bound U

$m = CalculateMeanGrayscale(\mathbf{I})$
for all pixel i in **I do**
  $\mathbf{p} = \mathbf{I}(i)$
  $p'_R = \max\left(\frac{g}{m} p_R, U\right)$
  $p'_G = \max\left(\frac{g}{m} p_G, U\right)$
  $p'_B = \max\left(\frac{g}{m} p_B, U\right)$
  $\mathbf{R}(i) = \mathbf{p}'$
end for

Output: image **R**

3 STORM - CONTINUING LOCALLY

3.1 Extension to a Local TMO

Global TMOs are fast, but for results of the highest quality local TMOs are used (Kuang et al., 2004; Kuang et al., 2007). Hence a natural direction of further Flash improvement is to extend it to a local version. One of the common approaches for such an extension is to perform tone mapping with pixel-based parameters, which are determined by looking only at the local area surrounding a given pixel instead of at the whole image (Reinhard et al., 2010). There is evidence that early stages of visual processing can be modelled by filtering of retinal image using filters of different scales (Wilson, 1991) and similar approaches have been used in various tone mapping and image enhancement methods (Peli, 1990; Jobson et al., 1997; Pattanaik et al., 1998). Thus the local extension of Flash proposed here does the same thing. If R and C are the number of image rows and columns, respectively, then let d be the smaller of these two i.e. $d = \min\{R, C\}$. For a pixel i Flash is applied to M squares of size $s_j d \times s_j d$ with pixel i in their center where s_j is the scaling factor for the j-th square. If k_j is the j-th square and $F_a^{(k_j)}(i)$ the value of luminance of pixel i after applying Flash$_a$ to k_j with i in its center, then the final luminance value for i is obtained as

$$S(i) = \frac{1}{M} \sum_{j=1}^{M} F_a^{(k_j)}(i). \tag{5}$$

The main computation cost of Eq. (5) is in calculating Eq. (4) for each i and k_j, which is effectively done by means of convolution over the luminance logarithms. Such an approach was motivated by the multiscale Retinex (MSR) algorithm (Jobson et al., 1997), but there are two differences. First, while MSR uses Gaussian kernels, having square kernels in Eq. (5) allows faster filtering by using a single integral image (Crow, 1984), which also brings the per-pixel complexity of Eq. (5) to $O(M)$. Second, unlike in MSR, there are no weights in Eq. (5) for individual kernels because using them has shown no significant benefit in terms of quality. The contribution of various kernels is shown in Fig 1. Like with Flash, higher values of a for Storm give better contrast in the final image as it is shown in Fig. 2. Since the proposed local TMO applies Flash multiple times and multiple flashes often occur during storms, it is named Storm for easier notation, while its application with n specified scaling factors and value of a for the underlying Flash is denoted Storm$_a^{(s_1,\ldots,s_n)}$. The pseudocode for Storm is given in Algorithm 2.

3.2 Properties

Fig. 1 shows how more kernels make more details visible. With well chosen kernels Storm outperforms Flash in terms of quality, but at the cost of the additional memory that is needed for the integral image.

In terms of complexity, Storm is also more complex than Flash. Firstly, Storm calculates the integral

(a) (b) (c) (d) (e)

Figure 1: Applications of Storm with different kernels followed by and Leap_{110} and gamma correction: (a) $\text{Storm}_{20}^{(1)}$, (b) $\text{Storm}_{20}^{\left(1,\frac{1}{4}\right)}$, (c) $\text{Storm}_{20}^{\left(1,\frac{1}{4},\frac{1}{16}\right)}$, (d) $\text{Storm}_{20}^{\left(1,\frac{1}{4},\frac{1}{16},\frac{1}{64}\right)}$, and (e) $\text{Storm}_{20}^{\left(1,\frac{1}{4},\frac{1}{16},\frac{1}{64},\frac{1}{256}\right)}$.

(a) (b)

Figure 2: Results of application of (a) $\text{Storm}_{1}^{\left(1,\frac{1}{4},\frac{1}{16}\right)}$ and (b) $\text{Storm}_{20}^{\left(1,\frac{1}{4},\frac{1}{16}\right)}$ to the same image.

Algorithm 2: Storm.

Input: image $\mathbf{I}$, brightening parameter a, M kernel sizes s_j, upper bound U

for all pixel i in $\mathbf{I}$ **do**
  $\mathbf{p} = \mathbf{I}(i)$
  $L = \max\{p_R, p_G, p_B\}$
  $L' = 0$
  for $j = 1$ **to** M **do**
    $L' = L' + F_a^{(k_j)}(i)$
  end for
  $\mathbf{R}(i) = \frac{L'}{L}\mathbf{p}$
end for
$\mathbf{R} = U \cdot \mathbf{R} / \max(\mathbf{R}(:))$

Output: image $\mathbf{R}$

image in $O(1)$ per-pixel complexity. Next, to each pixel Eq. (3) is applied M times and each time in $O(1)$ per-pixel complexity by using the integral image. Together this gives $O(M)$ per-pixel complexity, which seemingly violates the constraint set up in the introduction. However, M is supposed to be very small because already for $M \in \{2,3,4\}$ the results are of high quality. Additionally, since M can be considered a hyperparameter, once its value is chosen, it does not change that often so it is effectively a constant. Thus, taking all this into account, Storm can also be regarded as having $O(1)$ per-pixel complexity. Speed tests in Section 4.2 also corroborate such reasoning.

After carrying out subjective assessment of a large number of LDR images obtained by applying Storm and Leap, it was concluded that the combination with round default values that already produce visually appealing results without showing unrealistically too much details is $\text{Storm}_{20}^{\left(1,\frac{1}{4},\frac{1}{16}\right)}$+$\text{Leap}_{110}$.

4 EXPERIMENTAL RESULTS

4.1 Image Quality Metrics

The best way to the assess the quality of tone mapped images would be to carry out subjective perceptual studies. However, such studies were omitted here because they are time-consuming, they require special environment and carefully calibrated equipment, and they are not easy to reproduce. Instead, two objective measures are used: Feature Similarity Index For Tone-Mapped images (FSITM) (Ziaei Nafchi et al., 2015) and the already mentioned TMQI. TMQI-II was not used here because while images with a high TMQI-II are usually of high quality, a lot of images with a low TMQI-II are actually of high quality as well. This is because TMQI-II is too susceptible to mean grayscale value as shown in (Banić and Lončarić, 2016). FSITM is based on local phase information of images and it was shown

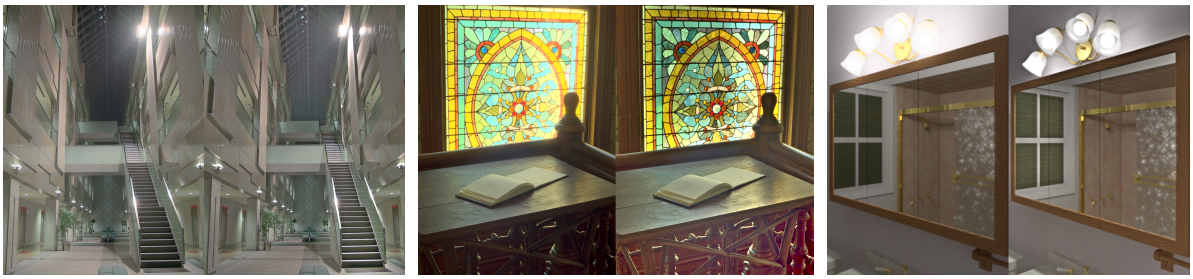

(a) (b) (c)

Figure 3: Pairwise comparison between the results of Reinhard's local TMO (Reinhard et al., 2002) on the left and Storm+Leap on the right; for Reinhard's TMO its Luminance HDR implementation with default parameter values was used.

Table 1: Mean TMQI and FSITM^G_TMQI obtained on images from (Ward, 2015) with cumulative execution time.

TMO	TMQI	FSITM^G_TMQI	t (s)
Ashikhmin (Ashikhmin, 2002)	0.6620	0.7338	225.23
Drago (Drago et al., 2003)	0.7719	0.8158	30.69
Durand (Durand and Dorsey, 2002)	0.8354	0.8405	225.14
Fattal (Fattal et al., 2002)	0.7198	0.7810	64.78
Mantiuk (Mantiuk et al., 2006)	0.8225	0.8266	88.03
Mantiuk (Mantiuk et al., 2008)	0.8443	0.8494	36.20
Pattanaik (Pattanaik et al., 2000)	0.6813	0.7635	46.91
Reinhard (Reinhard et al., 2002)	0.8695	0.8581	33.41
Reinhard (Reinhard and Devlin, 2005)	0.6968	0.7679	30.01
Flash_{10}	0.8072	0.8315	**21.19**
Flash_{10}+Leap_{110}	0.8755	**0.8625**	21.26
$\text{Storm}_{20}^{\left(1,\frac{1}{4},\frac{1}{16}\right)}$	0.7675	0.8004	24.35
$\text{Storm}_{20}^{\left(1,\frac{1}{4},\frac{1}{16}\right)}$+$\text{Leap}_{110}$	**0.8782**	0.8551	24.59

to give better results than TMQI. If combined with TMQI, it performs a better assessment than both TMQI and TMQI-II and this combination is denoted as FSITM^C_TMQI where C is a color channel. In this paper the green (G) color channel is used since it was shown to give good results (Ziaei Nafchi et al., 2015). All these measures are in range $[0,1]$ with a higher number meaning higher quality. These metrics are well established, easily reproducible, they have a sound theoretical background, their values can be calculated fast and automatically, and, all of them were shown to be well correlated with subjective measures.

4.2 Tone Mapping Quality and Speed

The quality of the results of the proposed TMO was evaluated by applying them to images in the HDR dataset given at (Ward, 2015). For TMOs with fixed parameters this dataset is challenging since it contains HDR images from different sources including artificially generated ones. Table 1 shows the obtained values of objective quality measures for the proposed and existing TMOs with default parameter values. For results of other TMOs the open source Luminance HDR software was used like in (Ma et al., 2015). This was also an opportunity to compare the proposed TMOs to easily available implementations of other well-known TMOs. The results for Flash differ from the ones given in (Banić and Lončarić, 2016) because here the gamma correction was carried out after tone mapping as it is supposed to be done. The values of objective metrics are higher for Flash and Storm than for all other tested TMOs and although the differences are small, they still demonstrate the quality of the proposed TMOs. Since Reinhard's local TMO (Reinhard et al., 2002) is considered to be among the best, in Fig. 3 its results are compared to the results of Storm.

Table 1 also shows that Flash and Storm are faster than other TMOs, which makes them good candidates for real-time applications.

5 CONCLUSIONS

A new TMO has been proposed in a global and local variant under the constraints of $O(1)$ per-pixel complexity and a practical design. Both variants were

shown to outperform state-of-the-art TMOs in terms of resulting LDR image quality even though obtaining high quality was only their secondary goal. Another important fact is that the proposed TMO was shown to be significantly faster than other TMOs. Its success demonstrates how having implementation constraints during the design phase of a TMO can nevertheless lead to fast and practical TMOs that also produce results of the highest quality. Additionally, the steps of the proposed TMO have their roots in the results of perceptual experiments. Future work will consider solutions that are less dependant on structures such as integral images in order to decrease TMO's memory consumption and to make it more hardware-friendly.

REFERENCES

Ashikhmin, M. (2002). A tone mapping algorithm for high contrast images. In *Proceedings of the 13th Eurographics workshop on Rendering*, pages 145–156. Eurographics Association.

Banić, N. and Lončarić, S. (2014a). Color Badger: A Novel Retinex-Based Local Tone Mapping Operator. In *Image and Signal Processing*, pages 400–408. Springer.

Banić, N. and Lončarić, S. (2014b). Improving the Tone Mapping Operators by Using a Redefined Version of the Luminance Channel. In *Image and Signal Processing*, pages 392–399. Springer.

Banić, N. and Lončarić, S. (2015). Smart Light Random Memory Sprays Retinex: a fast Retinex implementation for high-quality brightness adjustment and color correction. *JOSA A*, 32(11):2136–2147.

Banić, N. and Lončarić, S. (2016). Puma: A High-Quality Retinex-Based Tone Mapping Operator. In *Signal Processing Conference (EUSIPCO), 2016 24rd European*, pages 943–947. IEEE.

Banić, N. and Lončarić, S. (2017). Towards hardware-friendly Retinex algorithms. In *Image and Signal Processing and Analysis (ISPA), 2017 10th International Symposium on*, pages 104–108. IEEE.

Banić, N. and Lončarić, S. (2016). Sensitivity of Tone Mapped Image Quality Metrics to Perceptually Hardly Noticeable Differences. In *Proceedings of The Fifth Croatian Computer Vision Workshop (CCVW 2013)*, number 1, pages 15–18. University of Zagreb Faculty of Electrical Engineering and Computing.

Braun, G. J. and Fairchild, M. D. (1999). Image lightness rescaling using sigmoidal contrast enhancement functions. *Journal of Electronic Imaging*, 8(4):380–393.

Chiu, K., Herf, M., Shirley, P., Swamy, S., Wang, C., Zimmerman, K., et al. (1993). Spatially nonuniform scaling functions for high contrast images. In *Graphics Interface*, pages 245–245. CANADIAN INFORMATION PROCESSING SOCIETY.

Crow, F. C. (1984). Summed-area tables for texture mapping. *ACM SIGGRAPH computer graphics*, 18(3):207–212.

Dowling, J. E. (1987). *The retina: an approachable part of the brain*. Harvard University Press.

Drago, F., Myszkowski, K., Annen, T., and Chiba, N. (2003). Adaptive logarithmic mapping for displaying high contrast scenes. In *Computer Graphics Forum*, volume 22, pages 419–426. Wiley Online Library.

Durand, F. and Dorsey, J. (2002). Fast bilateral filtering for the display of high-dynamic-range images. *ACM transactions on graphics (TOG)*, 21(3):257–266.

Fairchild, M. D. (2015). http://rit-mcsl.org/fairchild/hdrps/hdrthumbs.html.

Fattal, R., Lischinski, D., and Werman, M. (2002). Gradient domain high dynamic range compression. In *ACM Transactions on Graphics (TOG)*, volume 21, pages 249–256. ACM.

Huang, J. and Mumford, D. (1999). Statistics of natural images and models. In *Computer Vision and Pattern Recognition, 1999. IEEE Computer Society Conference on.*, volume 1. IEEE.

Jobson, D. J., Rahman, Z.-u., Woodell, G., et al. (1997). A multiscale retinex for bridging the gap between color images and the human observation of scenes. *Image Processing, IEEE Transactions on*, 6(7):965–976.

Koschan, A. and Abidi, M. (2008). *Digital Color Image Processing*. Wiley.

Kuang, J., Yamaguchi, H., Johnson, G. M., and Fairchild, M. D. (2004). Testing HDR image rendering algorithms. In *Color and Imaging Conference*, volume 2004, pages 315–320. Society for Imaging Science and Technology.

Kuang, J., Yamaguchi, H., Liu, C., Johnson, G. M., and Fairchild, M. D. (2007). Evaluating HDR rendering algorithms. *ACM Transactions on Applied Perception (TAP)*, 4(2):9.

Larson, G. W., Rushmeier, H., and Piatko, C. (1997). A visibility matching tone reproduction operator for high dynamic range scenes. *Visualization and Computer Graphics, IEEE Transactions on*, 3(4):291–306.

Ma, K., Yeganeh, H., Zeng, K., and Wang, Z. (2015). High dynamic range image compression by optimizing tone mapped image quality index. *Image Processing, IEEE Transactions on*, 24(10):3086–3097.

Mantiuk, R., Daly, S., and Kerofsky, L. (2008). Display adaptive tone mapping. In *ACM Transactions on Graphics (TOG)*, volume 27, page 68. ACM.

Mantiuk, R., Myszkowski, K., and Seidel, H.-P. (2006). A perceptual framework for contrast processing of high dynamic range images. *ACM Transactions on Applied Perception (TAP)*, 3(3):286–308.

Meylan, L. and Susstrunk, S. (2006). High dynamic range image rendering with a retinex-based adaptive filter. *Image Processing, IEEE Transactions on*, 15(9):2820–2830.

Nguyen, R. M. and Brown, M. S. (2017). Why You Should Forget Luminance Conversion and Do Something Better. In *Proceedings of the IEEE Confe-*

rence on Computer Vision and Pattern Recognition, pages 6750–6758.

NTUST, C. G. G. (2015). http://graphics.csie.ntust.edu.tw/pub/hdr/.

Pattanaik, S. N., Ferwerda, J. A., Fairchild, M. D., and Greenberg, D. P. (1998). A multiscale model of adaptation and spatial vision for realistic image display. In *Proceedings of the 25th annual conference on Computer graphics and interactive techniques*, pages 287–298. ACM.

Pattanaik, S. N., Tumblin, J., Yee, H., and Greenberg, D. P. (2000). Time-dependent visual adaptation for fast realistic image display. In *Proceedings of the 27th annual conference on Computer graphics and interactive techniques*, pages 47–54. ACM Press/Addison-Wesley Publishing Co.

Peli, E. (1990). Contrast in complex images. *JOSA A*, 7(10):2032–2040.

Reinhard, E. and Devlin, K. (2005). Dynamic range reduction inspired by photoreceptor physiology. *Visualization and Computer Graphics, IEEE Transactions on*, 11(1):13–24.

Reinhard, E., Heidrich, W., Debevec, P., Pattanaik, S., Ward, G., and Myszkowski, K. (2010). *High dynamic range imaging: acquisition, display, and image-based lighting*. Morgan Kaufmann.

Reinhard, E., Stark, M., Shirley, P., and Ferwerda, J. (2002). Photographic tone reproduction for digital images. In *ACM Transactions on Graphics (TOG)*, volume 21, pages 267–276. ACM.

Schlick, C. (1995). Quantization techniques for visualization of high dynamic range pictures. In *Photorealistic Rendering Techniques*, pages 7–20. Springer.

Shapley, R. and Enroth-Cugell, C. (1984). Visual adaptation and retinal gain controls. *Progress in retinal research*, 3:263–346.

Tumblin, J. and Rushmeier, H. (1993). Tone reproduction for realistic images. *Computer Graphics and Applications, IEEE*, 13(6):42–48.

Tumblin, J. and Turk, G. (1999). LCIS: A boundary hierarchy for detail-preserving contrast reduction. In *Proceedings of the 26th annual conference on Computer graphics and interactive techniques*, pages 83–90. ACM Press/Addison-Wesley Publishing Co.

Urbano, C., Magalhães, L., Moura, J., Bessa, M., Marcos, A., and Chalmers, A. (2010). Tone mapping operators on small screen devices: an evaluation study. In *Computer Graphics Forum*, volume 29, pages 2469–2478. Wiley Online Library.

Ward, G. (1994). A contrast-based scalefactor for luminance display. *Graphics gems IV*, pages 415–421.

Ward, G. (2015). http://www.anyhere.com/gward/hdrenc/pages/originals.html.

Wilson, H. R. (1991). Psychophysical models of spatial vision and hyperacuity. *Spatial vision*, 10:64–81.

Yeganeh, H. and Zhou, W. (2013). Objective Quality Assessment of Tone Mapped Images. *Image Processing, IEEE Transactions on*, 22(2):657–667.

Ziaei Nafchi, H., Shahkolaei, A., Farrahi Moghaddam, R., and Cheriet, M. (2015). FSITM: A Feature Similarity Index For Tone-Mapped Images. *Signal Processing Letters, IEEE*, 22(8):1026–1029.